Atmos. Chem. Phys. Discuss., 12, 7909–7947, 2012
www.atmos-chem-phys-discuss.net/12/7909/2012/
doi:10.5194/acpd-12-7909-2012

Atmospheric Chemistry and Physics Discussions

Effects of ice crystals on the FSSP measurements in mixed phase clouds

G. Febvre[1], J.-F. Gayet[1], V. Shcherbakov[1,2], C. Gourbeyre[1], and O. Jourdan[1]

[1]Laboratoire de Météorologie Physique, UMR6016 CNRS/Université Blaise Pascal, Clermont-Ferrand, France
[2]LaMP, Institut Universitaire de Technologie d'Allier, Montluçon, France

Received: 24 February 2012 – Accepted: 6 March 2012 – Published: 20 March 2012

Correspondence to: G. Febvre (guy.febvre@opgc.univ-bpclermont.fr)

Published by Copernicus Publications on behalf of the European Geosciences Union.

Abstract

In this paper, we show that in mixed phase clouds FSSP-100 measurements may be contaminated by ice crystals, inducing wrong interpretation of particle size and subsequent bulk parameters. This contamination is generally revealed by a bimodal feature of the particle size distribution; in other words, in mixed phase clouds bimodal features could be an indication of the presence of ice particles. The combined measurements of the FSSP-100 and the Polar Nephelometer give a coherent description of the effect of the ice crystals on the FSSP-100 response. The FSSP-100 particle size distributions are characterized by a bimodal shape with a second mode peaked between 25 and 35 µm related to ice crystals. This feature is observed with the FSSP-100 at airspeed up to 200 m s^{-1} and with the FSSP-300 series. In order to assess the size calibration for clouds of ice crystals the response of the FSSP-100 probe has been numerically simulated using a light scattering model of randomly oriented hexagonal ice particles and assuming both smooth and rough crystal surfaces. The results suggest that the second mode measured between 25 µm and 35 µm, does not necessarily represent true size responses but likely corresponds to bigger aspherical ice particles. According to simulation results, the sizing understatement would be neglected in the rough case but would be major with the smooth case. Qualitatively, the Polar Nephelometer phase function suggests that the rough case is the more suitable to describe real crystals. Quantitatively, however, it is difficult to conclude. Previous cloud in situ measurements suggest that the FSSP-100 secondary mode, peaked in the range 25–35 µm, is likely to be due to the shattering of large ice crystals on the probe tips. This finding is supported by the rather good relationship between the concentration of particles larger than 20 µm (hypothesized to be ice shattered-fragments measured by the FSSP) and the concentration of (natural) ice particles larger than 100 µm (CPI data). The shattering efficiency is defined as the ratio of the measured ice shattered-fragments to the number of natural ice particles (with $d > 100$ µm) impacting the probe leading edge. In the present study the shattering efficiency is evaluated to ~7 %. It is found that about

ACPD

12, 7909–7947, 2012

400 ice fragments may result from the shattering of one equivalent irregular shaped ice crystal with a mean volume diameter of 310 µm. Obviously, these values could be strongly dependent on the inlet design, the airspeed and the robustness of ice crystals via the impact kinetic energy to surface energy ratio providing the particle breakup.

1 Introduction

Investigations for climate, radiative transfer or numerical forecast modelling require a good knowledge of the microphysical properties of clouds. In situ measurement science uses quantitative types of probes in order to perform the particle size analysis of hydrometeor range going from a few microns to a millimetre. One such classic probe is the FSSP, designed to count cloud droplets individually in different size ranges. The particle size is determined from the measured light intensity using Mie scattering theory (Knollenberg, 1970, 1981). There are many applications where FSSP is used especially when accurate measurements of cloud liquid water content (LWC) and droplet spectra are required. Cober et al. (1995, 1999), based on works of Ashenden and Marwitz (1998) and Miller et al. (1998), give as an example of FSSP use, the case of aircraft icing characterizations. The LaMP's activities in the area of aircraft icing and the implication of the FSSP in these studies give motivation to explore any situation capable of increasing the knowledge of FSSP behaviour. This is useful mainly in order to calculate bulk parameter such as the liquid water content (LWC) and mean volume diameter (MVD) with minimum errors.

The scientific community of cloud physics (see the recent review on cloud in situ instruments by Baumgardner et al., 2011) seems to agree that the FSSP is a suitable probe only when the liquid phase is present, even if the discussion is not closed concerning the quantification of uncertainties in the evaluation of the LWC. Nagel et al. (2007) showed, with a rigorous calibration method, that a sizing accuracy of about 10 % can be expected.

ACPD
12, 7909–7947, 2012

The interpretation of the measurements is quite complicated in the presence of ice particles, and becomes more so if recent results concerning the shattering effects are considered (Jensen et al., 2009). Gardiner and Hallett (1985) suggested that the FSSP gives a false response in ice clouds and should not be used for the characterization of small ice crystals. Since then Gayet et al. (1996) compared the PMS cloud probe (2D-C) and FSSP size distributions in the poorly measured overlap region and proposed that observations made with the FSSP probe can be considered reliable if the ice crystals are small and spherical. In such cases there is indeed good agreement between the 2D-C and FSSP. Ivanova et al. (2001) suggest, comparing the FSSP and the DRI Cloudscope spectra, that errors due to aspherical effects appear marginal when radiative properties are calculated. Mitchell et al., 1999 found similar good agreement when hexagonal plates were sampled, using the same experimental design.

Even if the sizing of ice crystals seems reliable with FSSP measurement in some particular situations (i.e. spherical particles, Gayet et al., 1996), the size response should consider specific theoretical methods adapted for aspherical particles (see for instance Borrmann et al., 2000). In lots of situations, clouds with mixed phase (liquid water droplets and ice crystals) introduce risks for misinterpretation if differentiation between the two hydrometeor phases is not possible. As Riley (1998) states, the problem would not be important if mixed conditions were rare, but mixed phase clouds are a common situation. In his review, this author found that mixed-phase conditions in clouds were observed with a frequency of between 20 % and 90 %, depending on the region, environment, and temperature.

Cober et al. (2001) present an interesting discussion for the responses of several common instruments in mixed-phase situations. The conclusion always seems to be similar namely that it is difficult to evaluate the contribution of each phase in a measurement. In the case of the FSSP, the presence of ice particles could lead to a wrong evaluation of cloud parameters such as liquid water content (LWC) and mean volume diameter (MVD).

ACPD
12, 7909–7947, 2012

This paper is a contribution to the interpretation of the effects of ice particles on FSSP measurements in Arctic mixed-phase clouds. The data discussed, were obtained during the ASTAR 2007 (Arctic Study on Tropospheric Aerosol and Radiation, Engvall et al., 2008) and POLARCAT (Polar Study using Aircraft, Remote Sensing, Surface Measurements and Models, of Climate, Chemistry, Aerosols, and Transport, Law et al., 2008) field experiments. During ASTAR, the cloud observations were carried out onboard the Polar2 (Do228) operated by AWI (Alfred Wegener Institute for Polar and Marine Research) whereas the ATR42 research aircraft operated by SAFIRE (Service des Avions Français Instrumentés pour la Recherche en Environnement) was used during POLARCAT. A combination of cloud in situ instruments was installed on both aircraft, namely: a standard Forward Scattering Spectrometer Probe (FSSP-100), a Polar Nephelometer (Gayet et al., 1997), as well as a Cloud Particle Imager (CPI, Lawson et al., 2001) to measure cloud particle properties in terms of scattering, morphology and size, and in-cloud partitioning of ice/water content. Standard 2D-C, 2D-P instruments as well as Liquid water devices (i.e. King probe, Nevzorov and PVM-100) completed the ATR42 in situ cloud instrumentation.

A short description of the instruments and the analysis of cloud situations are first presented in Sect. 2. Then the paper describes in detail the FSSP response in the presence of ice particles (Sect. 3). A presentation of the microphysical and optical properties of a mixed-phase boundary-layer cloud observed during the 8 April 2007 situation (ASTAR) will then be given. The interpretation of the measurements from independent techniques leads to a clear identification of the effects of ice crystals on FSSP particle size distributions. This feature is confirmed with the extended data obtained during POLARCAT, studied in order to experience a wide range of ice crystal conditions. Section 4 discusses the implications on FSSP measurements and Sect. 5 attempts to evaluate the ice shattering efficiency.

ACPD
12, 7909–7947, 2012

2 Instrumentation and cloud situations

The cloud instrumentation installed onboard the Polar2 and ATR42 aircraft has been thoroughly described by Gayet et al. (2009). We recall that it includes three independent techniques for the description of particles within a diameter range varying from a few micrometers (typically 3 µm) to about 2 mm: (1) the PMS FSSP-100 probe, (2) the Cloud Particle Imager (CPI) and (3) the Polar Nephelometer. The accuracies of measurements could be hampered by the shattering of ice crystals on probes with shrouded inlet (FSSP, CPI, Polar Nephelometer, 2D-C, ... for instance, see among others Heymsfield, 2007). Experimental evidence shows that for particle diameters larger than about 100 µm, the number of shattered particles increases with the concentration of large particles. The new generation of cloud instruments (CDP, CIP, 2D-S, ...) are equipped with innovative shrouded inlets specially designed to reduce the shattering effects (Korolev et al., 2011) and provide information to separate real and artifact-shattered crystals (Field et al., 2003, 2006). As these instruments were unavailable for the present study, the effects of resulting ice-crystal shattering will be discussed together with the results below.

The FSSP-100 instrument provides information on droplet size distribution for the size range of 2–47 µm (Baumgardner et al., 2002). The accuracies of the derived effective diameter and liquid water content have been estimated as 2 µm and 30 %, respectively. Referring to the effects of ice crystals shattering on FSSP data, the bulk parameters could be overestimated by about 15–20 % (Heymsfield, 2007) and the particle concentration by a factor of 2 or 3 (Field et al., 2003). Similar measurement uncertainties due to shattering effects are expected for CPI data (see below).

The CPI registers cloud-particle images on a solid-state, one-million pixel digital charge-coupled device (CCD) camera by freezing the motion of the particle using a 40 ns pulsed, high-power laser diode (Lawson et al., 2001). A particle detection system with upstream lasers defines the focal plane so that at least one particle in the image is in focus. Each pixel in the CCD camera array has an equivalent size in the

ACPD
12, 7909–7947, 2012

sample area of 2.3 µm, so particles of sizes ranging from approximately 10 µm to 2 mm are imaged. In a previous paper (Gayet et al., 2009), conclusive comparisons between CPI and PMS 2D-C/2D-P particle size distributions during POLARCAT were shown. These results validate the CPI calibration as well as the data processing method and suggest that the errors on the size distributions and derived microphysical parameters calculated from the (calibrated) CPI are of the same order as those from the PMS instruments.

The Polar Nephelometer (Gayet et al., 1997) measures the scattering phase function of an ensemble of cloud particles (i.e., water droplets or ice crystals or a mixture of these particles ranging in size from a few micrometers to about 1 mm in diameter). Direct measurement of the scattering phase function allows the discrimination of particle shapes (spherical liquid water droplets or aspherical ice crystals) and the calculation of integrated optical parameters (such as extinction coefficient and asymmetry parameter (g), see Gayet et al., 2002).

Indeed, Sassen et al. (1979) proposes an identification of phase clouds on the basis of their side scattering differences with water or ice particles. With this idea, the phase function measured from Polar Nephelometer (PN) could be used to separate the phase of hydrometeor. Crépel et al. (1997) present a method of liquid or ice discrimination based on the comparison between scattered power from two different side angles: 113° and 141° (rainbow peak). By using a shape criterion of the phase function as the asymmetry factor, discrimination between water droplets or ice crystals is possible. Zang et al. (2007) show different theoretical values of g ranging from 0.87 for ice spheres to 0.6 for polyhedrons at a wavelength of 0.66 µm. Gayet et al. (2002) show that results from PN measurements indicate g-values ranging from 0.86 to 0.75 for water droplets and ice crystals respectively; this result is in good agreement with those obtained by Garrett et al. (2001).

In this study, the PN phase function shape (through the asymmetry parameter) will be used in order to discriminate the phase of the cloud particles. The accuracies of the extinction coefficient and asymmetry parameter derived from the Polar Nephelometer are estimated to be within 25 % and ±0.05, respectively (Jourdan et al., 2010). These measurement uncertainties could be affected by ice-crystal shattering on the probe inlet (Shcherbakov et al., 2010).

The situations presented below all address Arctic boundary layer mixed-phase stratiform clouds. They exhibit a cloud top layer dominated by liquid-water in which ice precipitation was yielded. This is a common feature observed in such clouds (McFarquhar et al., 2007) even for cloud top temperatures down to −25 °C during ASTAR and POLARCAT. Generally, very efficient ice growth processes are expected in boundary layer clouds since appreciable liquid water is converted into ice water with large precipitating ice crystals. During ASTAR, the flights were carried out over the Greenland Sea in the vicinity of the west coast of the Svalbard Archipelago whereas the POLARCAT flights were planned over the Greenland Sea towards Northern parts of the Scandinavian Peninsula.

3 Evidence of the FSSP response to ice crystals

3.1 The problems of ice crystal detection

The sizing principle of the FSSP is based on the measurement of the scattered light between 3 and 15° by a single particle. Indeed, for spherical particles, Mie theory gives a relation between scattered energy and particle size. Based on such calculations, the measured intensities are interpreted as particle sizes by the probe electronics (Pinnick et al., 1981). As a consequence, for a nominal hydrometeor sizing, the calibration curve (i.e. the relationship between measured scattered intensities and sizes) of the FSSP is extremely important. Usually, water liquid spheres are used in Mie calculations. As a consequence, particles with aspherical shape could present significant differences in scattering properties, especially in terms of scattering light power as a function of scattering angle. In others words, the phase function (angular distribution of diffuse energy) is sensitive to the morphological characteristics of the lighted particle (see for instance examples of Polar Nephelometer measurements, Gayet et al., 1998). For the same geometric volume, aspherical particles scatter between 3° and 15° a light power that differs from those predictable using Lorentz-Mie theory (Borrmann et al., 2000). Thus, the size ranging can be affected, leading to uncertainties in the bulk parameter calculation and mean diameter.

In order to minimize uncertainties, several techniques combining different instruments have been used. For example Niu (2008) used Icing Rosemount probe data in order to define a threshold for removing the noise due to ice contamination of the FSSP data. This approach is usable in mixed cloud conditions to isolate liquid water zones, but reliable measurements are lost in the presence of a high concentration of ice crystals.

To resume, FSSP measurements could be contaminated by ice crystals, inducing a wrong interpretation of the particle size and subsequent bulk parameters. Discrimination of liquid water clouds and mixed or iced cloud is a great challenge for a correct FSSP measurements analysis, but a hazardous process if only the FSSP probe is available.

Conversely, the shape of the spectra in the presence of ice particles may be a good indication of the presence of ice crystals. In this study, we will demonstrate below that the bimodal shape spectrum is undoubtedly the signature of ice crystals in mixed-phase clouds. Literature sometimes describes a typical behaviour of the FSSP in the presence of ice (mixed or iced clouds).

3.2 The case study of the 8 April 2007 (ASTAR)

Figure 1 displays the time-series of cloud parameters measured during a descent-climbing sequence in the mixed-phase stratiform cloud layer and yielded precipitations during the 8 April 2007 case study (ASTAR 2007 experiment). The parameters (plotted at 1 Hz, i.e. 70 m horizontal resolution) are the following: the air temperature, altitude, droplet concentration, liquid water content (LWC) and mean volume diameter (MVD) inferred from FSSP-100, the concentration of ice particles larger than 100 µm ($C100$

ACPD
12, 7909–7947, 2012

from the CPI), the asymmetry parameter (g from the Polar Nephelometer) and finally the FSSP size distribution represented by a coloured scale of the particle concentration. Without bulk water probe information during ASTAR, the consistency of the FSSP measurements was verified in liquid water clouds (i.e. $g > 0.83$) by comparing the extinction coefficient derived from the Polar Nephelometer data. The results displayed on Fig. 2 show that the slope parameter (0.95) is close to a perfect agreement and the dispersion of the data points (20 %) is within the probe uncertainties. The descent-climbing sequence provides the vertical profiles of LWC, MVD, g and $C100$ as displayed on the four panels on Fig. 3. The results show that liquid water droplets dominate the cloud microphysical and optical properties in the upper parts of the cloud from 600 m/−16 °C to 1200 m/−20 °C (LWC up to 0.3 g m^{-3}) as confirmed by the asymmetry parameter values ranging from 0.830 and 0.855. The $C100$ profile indicates that ice particles are found even near the cloud top with rather a low concentration (∼5 l^{-1}), which then significantly increases (up to ∼40 l^{-1}) at lower levels, with g-values of about 0.77.

3.3 Evidence of the FSSP response to ice crystals

In order to evidence the FSSP response to ice crystals we have selected four time-sequences which are marked on the time-series on Fig. 1 by shadowed areas. Sequence a addresses the top of the cloud layer where mostly liquid water droplets are detected. Sequences b and c correspond to mixed-phase conditions (water droplets and ice crystals) and the last sequence (d) relates precipitating ice crystals only. In order to achieve the statistical representativeness of the results, the length of the flight paths have been chosen according to particle concentration, i.e. by considering averages over 10 s. for the first sequence, 20 s. in mixed-phase conditions and 120 s. for the bottom part with a very low concentration. Table 1 summarises the corresponding main values of the microphysical and optical parameters with temperatures and altitudes.

ACPD
12, 7909–7947, 2012

Figure 4 (left panels) displays the mean particle size distribution (PSD) from FSSP and CPI measurements with some examples of ice crystal images for these four selected cloud sequences. The left panels of Fig. 4 represent the corresponding measured scattering phase function from the Polar Nephelometer (red dot symbols on the right panel). The theoretical phase function is calculated from the FSSP data using Mie theory (spherical water droplets) and plotted with black cross symbols. The PSD displayed on Fig. 4a is typical of a cloud of liquid-water droplets. The close agreement between the PN measurements and the theoretical FSSP-100 values confirms this statement (seen as already on Fig. 2). Near the cloud top the particle phase is dominated by (spherical) liquid water droplets even if some ice crystals are detected (see Table 1 and Fig. 4a) as reported by Gayet et al. (2009). Fig. 4b and c, which correspond to mixed phase cloud, show that the FSSP particle size distributions exhibit a bimodal shape with a second mode peaked near 30 µm. The amplitude of the second mode and the ration (REX) seem to be correlated ; when the latter increases, the former shows a similar tendency. We define REX as the ratio of extinction due to ice particles alone (CPI data) to the total extinction (water droplets and ice crystals, PN measurements). Conversely, the difference between the measured (PN) and theoretical (FSSP-100) phase functions at sideward scattering angles increases with REX values (see Table 1). This feature undoubtedly reveals the occurrence of aspherical particles with highly irregular shapes as exemplified on Fig. 4b and c. In the precipitating ice particles zone (Fig. 4d), the second mode of the PSD is strongly marked whereas simulated and measured phase functions are no longer comparable.

To summarize, the combined measurements of the FSSP and Polar Nephelometer give a coherent description of the effect of the ice crystals on the FSSP response. The second FSSP mode in the range 25–35 µm is undoubtedly a signature of ice crystals, which is more marked as the ice crystals are more dominating the cloud extinction properties. This feature seems to be a recurrent observation (Gardiner et al., 1985, Cober et al., 1995, Crépel et al., 1997) and more recently such typical size spectra have been reported by Gayet et al. (2009, see their Fig. 4b).

In order to generalise these observations, the combined data sets in mixed-phase clouds from ASTAR 2007 and POLARCAT experiments are used. During these two experiments, both the FSSP and Polar Nephelometer data were processed over 1Hz frequency and represent about 30 000 available measurements. Two parameters have been defined to characterize the second mode of the particle size distribution and the scattering phase function, i.e. the mean volume diameter (from the FSSP) and the asymmetry parameter (PN data). Figure 5 displays the g-MVD scatter plots of the 30000 measurements. The results show that two main domains (labelled A and B) can be identified and are representative of two different cloud properties. The A domain, with MVD and g centered on 35 µm and 0.78 respectively, represent a typical ice particle population, whereas domain B (MVD and g centred on 10 µm and 0.84) is related to typical liquid water droplet clouds. We note on Fig. 5 that only a few data points are observed between the two main domains A and B. This feature is typical of Arctic mixed-phase clouds. Indeed, this confirms that these clouds have the liquid fraction (fl, i.e. the ratio of liquid water on the total water: liquid + ice) fl <0.2 or fl >0.8, with very few values in between (i.e., clouds were either dominated by liquid or ice, but few clouds had relatively equal contributions of ice and water) as already observed by Cober et al. (2001); Korolev et al. (2003) and MacFarquhar et al. (2007). The next section will discuss the implications of the presence of ice particles on FSSP measurements

4 Implications on FSSP measurements in mixed-phase and ice clouds

Our results clearly show that the second mode in the range 20–35 µm of the FSSP-100 size distribution is related to the presence of ice particles. It should be noticed that a similar feature is observed with the FSSP-300 instrument. Indeed, Fig. 6a displays particle size distributions simultaneously measured in a stratiform mixed-phase cloud by both FSSP series 100 and 300 on the ATR42 aircraft (POLARCAT Summer experiment). The results above have been obtained from airborne measurements performed

ACPD
12, 7909–7947, 2012

by twin-engine aircraft (Do228 and ATR42) with airspeed ranging from 80 to 100 $m\,s^{-1}$. It should be highlighted that a similar feature has already been obtained with the same FSSP-100 instrument but with higher airspeed (~200 $m\,s^{-1}$) onboard the DLR Falcon during the AEROCONTRAIL experiment (Gayet et al., 1998). Figure 6b displays typical FSSP size distributions measured during ASTAR and AEROCONTRAIL experiments showing a smaller secondary mode at high airspeed measurements (25 µm against 35 µm). Lawson (2011) also reported a secondary mode on FSSP measurements carried out at high airspeed (~200 $m\,s^{-1}$ with the DC8 NASA aircraft) in cirrus clouds (see his Fig. 10). Therefore a common feature is observed in the presence of ice crystals regardless of the probe version and airspeed.

It is difficult to give a satisfactory interpretation of this particular shape of the FSSP dimensional spectra. Gardiner and Hallett (1985) concluded that the mechanism for the response of the FSSP to ice particles is not well understood. A more critical aspect that could be considered is the probe size response to aspherical particles. Theoretically, the interpretation of the FSSP measurements draw up on the knowledge of the scattering phase function of sampled particles. Indeed, although modelling and measurement means are the norm, the use of only one aspherical particle randomly oriented in the laser beam is rarely considerd and is thus poorly documented. Shcherbakov et al. (2006) showed a good agreement between phase function measurements and modeling of a single ice particle from observations carried out during the South Pole Ice Crystal Experiment. The model was designed in order to take into account the particle orientation in the laser beam.

Considering the modeling of an ensemble of ice crystals, FSSP-300 size bins were defined from T-matrix calculations by Borrmann et al. (2000) assuming randomly oriented aspherical (i.e. rotationally symmetric ellipsoid) particles with an aspect ratio of 1:2. The upper size limits were found to be 18.0 µm and to be 16.1 µm for ice spheres and aspherical ice particles, respectively (Gayet et al., 2011). A closure method was used in order to validate the proposed FSSP-300 size calibration by comparing the extinction coefficients derived from the Polar Nephelometer and the FSSP-300.

ACPD
12, 7909–7947, 2012

We propose in the next section a theoretical FSSP-100 size calibration for ice crystals assuming hexagonal particles.

4.1 Theoretical FSSP-100 size calibration to ice crystals

In order to assess the size calibration for clouds of ice crystals, the response of the FSSP-100 probe with forward scattering aperture from 3° to 15° was numerically simulated using a light scattering model of randomly oriented hexagonal ice particles. More specifically, we employed the improved geometrical optics method (IGOM) developed by Yang and Liou (1996, 1998). The IGOM uses the ray-tracing technique to solve the near field on the ice crystal surface, which is then transformed to the far field on the basis of the electromagnetic equivalence theorem. Accordingly, the method can be applied to the computation of the extinction cross section for ice crystals with size parameters along the minimum dimension as small as ∼6, and of the phase function when size parameters along the minimum dimension are larger than ∼20 (Yang and Liou, 1996), that is, about 1.2 µm and 4 µm, respectively, for the FSSP wavelength of 632.8 nm. Basically, surface roughness is treated by assuming that a particle surface is composed of small facets that can be randomly tilted, and subsequently sampled for different realizations whereupon the amount of tilt follows a Gaussian distribution (Yang and Liou, 1998).

We performed our simulations for the roughness scale parameter $\sigma = 0$ and $\sigma = 0.2$. We recall that surface roughness tends to smooth out peaks and peculiarities, leading to smoother phase functions. Indeed the signature of particle shape is less visible on phase function when the particles are rough. These two σ chosen values give, firstly, crystals with perfect plane surfaces and secondly, crystals with very deep rough surfaces. We can expect to span the complete domain of the rough influence.

The responses of the FSSP-100 probe, i.e., scattering cross-sections viewed by the probe were computed considering forwardscattering between 3 to 15° with a refractive index $m = 1.3084 + i\,1.09.10^{-08}$ of ice at the wavelength $\lambda = 0.6328$ microns (Warren and Brandt, 2008) for hexagonal ice crystals having the aspect ratio of 0.5 and 2.0,

Discussion Paper | Discussion Paper | Discussion Paper | Discussion Paper |

ACPD

12, 7909–7947, 2012

Effects of ice crystals on the FSSP measurements in mixed phase clouds

G. Febvre et al.

namely, plates and columns.

The response presented here is the resulting scattering cross-sections as a function of the surface equivalent diameter in accordance with Mishchenko et al., 1997 when wavelength is small compared to particle size.

The resulting scattering cross-sections as a function of the surface equivalent diameter with the Mie theory calculations (for spherical particles of the water refractive index) are represented on Fig. 7. As for the FSSP-100 results (Fugal et al., 2009), with same measured cross-sections, the surface equivalent diameters for smooth hexagonal ice crystals are twice as big as the corresponding water droplet diameters. In the case of rough crystals, the difference between water and ice is very small. With same measured cross-sections, the surface equivalent diameters for rough hexagonal ice crystals are smaller than the corresponding water droplet diameters.

Therefore, considering the nominal calibration for water droplets, the size response for hexagonal ice crystals can be derived. In a similar way to Baumgardner et al. (1992) and Borrmann et al. (2000) the bin limit sizes of the FSSP-100 are given in Table II considering both standard size range (3–45 µm) and extended range (6–90 µm) and considering both types of ice crystal, smooth and rough. Of course the above results could only be considered as an assessment of the size response of the FSSP-100 to irregular ice crystals such as those observed in mixed-phase clouds. Nevertheless, a theoretical sensitivity study with different particle aspect ratios ranging from 0.5 to 2.0 shows that the subsequent effects on the theoretical results are no larger than 15 %. The rough aspect seems to play the crucial role in scattering studies. The difference between water and smooth ice crystal calibration is extremely large with an influence on the channel width. On the contrary, the scattering properties of a crystal with a deep roughness are very close to the spherical model.

Coming back to the observations in mixed-phase clouds we may suggest that the second mode, peaked between 25 µm and 35 µm, does not represent true size response but most likely corresponds to much bigger ice particles (i.e. 55 µm–86 µm) if we consider the calibration results above valid for smooth hexagonal particles. The

Discussion Paper | Discussion Paper | Discussion Paper | Discussion Paper |

ACPD

12, 7909–7947, 2012

Effects of ice crystals on the FSSP measurements in mixed phase clouds

G. Febvre et al.

smooth hexagonal particles model is probably not an adequate modelisation of real crystals. Size results obtained from this hypothesis represent the upper limit of real size. Real crystal sizes probably between those calculated from this hypothesis and the spherical or rough model.

The examination of the Polar Nephelometer phase function and crystal pictures (Fig. 4) confirm quantitatively the presence of rough crystals rather than smooth crystals. Qualitatively however it is difficult to conclude as the PN phase function does not show peaks (halos...) characteristic of smooth particles. Sensitivity studies deserve to be carried out in, this domain, although remain outside the scope of this paper.

4.2 Effects of ice crystals on FSSP measurements

In order to assess the maximum effects of ice crystals on the FSSP derived parameters, the contribution on number concentration, extinction and liquid/ice water content of the ice particles larger than 24 µm has been evaluated assuming the size calibration reported on Table II. The corresponding values have been scaled by the values calculated over the full FSSP size range assuming water droplets for particles smaller than 24 µm and smooth and rough ice particles for larger sizes. The results are reported on Figs. 8a (rough) and b (smooth) with the ratio values (called DELTA in %) as a function of the REX extinction ratio (CPI data to PN measurements, see definition in Sect. 3.3) and the asymmetry parameter, respectively. The data have been obtained for the four selected cloud sequences labelled a, b, c and d on Fig. 1.

In the rough condition, the volume parameter is the most affected by the contribution of ice particles. For REX values smaller than 0.2, DELTA is no larger than 25 %, 10 % and 5 % for the volume, surface and concentration measurements, respectively. At the same time the asymmetry parameter remains within a deviation of 0.01 (Fig. 8b). In this case the FSSP size distribution is hardly affected by the presence of ice crystals. When REX reaches about 0.4 with a subsequent g-decrease of 0.04 (0.80) the effects of ice crystals become significant (35 % and 65 % on the surface and volume, respectively). For larger DELTA values, the ice crystals control the FSSP size distribution.

ACPD
12, 7909–7947, 2012

In the smooth condition, the behaviour described previously is also observed, with a greater deviation until the REX parameter rises above 0.1. For volume parameter, Delta is equal to 70 % as soon as the presence of ice is detected.

This observation shows that complete interpretation of the FSSP measurements in the presence of ice crystals (ice cloud or mixed cloud) is not possible without an adequate modelisation of scattered light by ice crystals. Probes such as the polar nephelometer are in this case precious allies of all probes based on forwardscattering light measurements (i.e. FSSP or CDP Probes).

5 An attempt to evaluatethe ice shattering efficiency

If we now consider the origins of the FSSP-100 secondary mode there are three possibilities: (i) The small ice particles in the size range 20–35 µm are real; (ii) these ice crystals are due to the shattering of large ice crystals on the probe tips, and (iii) the combination of (i) and (ii). There is still considerable discussion regarding the magnitude of the contribution of the small ice crystals to the concentration and bulk microphysical parameters. Korolev and Isaac (2005), Lawson et al. (2006) and Protat et al. (2010) suggested that small ice crystals do contribute significantly to bulk microphysical properties. In relatively extreme situations, Heymsfield (2007) shows that shattering effects could add about 15 % to the ice water content from the FSSP, while the problem is even greater for extinction and number concentration. Field et al. (2003) and McFarquhar et al. (2007) confirm that shrouded inlets may cause particle shattering with a subsequent enhancement of the total concentration of ice crystals, especially at $D < 50$ µm. For particle diameters larger than about 100 µm, the number of shattered particles increases with the concentration of large particles.

There are no means of discriminating real and artefact ice particles related to the FSSP-100 secondary mode. However, following convincing results from measurements carried out using cloud probes with new inlets specially designed to reduce shattering effects (Korolev et al., 2011), the FSSP-100 secondary mode peaked in the range 25–35 µm is likely to be caused by the shattering of large ice crystals on the probe tips. Figure 9 gives convincing arguments showing that the number concentration of particles larger than 20 µm (hypothesized to be ice shattered-fragments measured by the FSSP) is related to the concentration of (natural) ice particles larger than 100 µm (CPI data). We note in passing that the data on Fig. 8 correspond to the sampling sequence of the lowermost cloud parts (from 10:58 to 11:06 UT, see Fig. 1) where only precipitating ice particles were observed. We define the shattering efficiency as the ratio of the ice shattered-fragments detected by the FSSP to the number of natural ice particles (with $d > 100$ µm) impacting the probe leading edge. Therefore, we may evaluate the shattering efficiency as follows:

First consider, as an example, a cloud with a real ice crystal size-distribution as presented on the Fig. 9a with a MVD of 310 µm and a total concentration of particles larger than 100 µm of 20 l^{-1}. The shattering efficiency is evaluated by assuming the surface of the leading edge of the FSSP sample tube on which the impacting ice crystals shatter and disperse. Considering outer and inner diameters of 4.5 cm and 3.8 cm, respectively the impinging surface is 4.5 cm^2 and the corresponding swept volume is 45 $l\,s^{-1}$ for the airspeed of 100 $m\,s^{-1}$. The rate of impacting ice particles ($d > 100$ µm) is therefore estimated at 900 s^{-1} considering the number concentration of ice particles ($d > 100$ µm) of 20 l^{-1}. Considering now the volume swept by the FSSP sampling surface (at 100 $m\,s^{-1}$) of 45 $cm^3\,s^{-1}$, the number of ice fragments counted by the FSSP-100 is 67 s^{-1} for a concentration of particles ($d > 20$ µm) of 1.5 cm^{-3} (see the CFSSP20-CCPI100 relationship on Fig. 9). In other words, 900 s^{-1} (natural) ice particles (with $d > 100$ µm) impacting the FSSP leading edge are shattered with a rate of ice fragments of 67 s^{-1} counted by the FSSP, resulting in a shattering efficiency of 67/900 ∼7 %.

Assuming now that the shattered fragments have the same probability of distribution along the cross-section of the FSSP tube, the fragmentation rate (i.e. the number of ice fragments related to the natural ice crystal population) may be evaluated. Indeed, considering 67 s^{-1} shattered ice fragments measured over the FSSP sampling surface of 0.44 10^{-2} cm^2 (see above), the total number of shattered fragments over the

Discussion Paper | Discussion Paper | Discussion Paper | Discussion Paper |

ACPD

12, 7909–7947, 2012

Effects of ice crystals on the FSSP measurements in mixed phase clouds

G. Febvre et al.

cross-section of the FSSP sample tube (11.4 cm^2) is : $67 \times 11.4\ 10^2/0.44 = 174\ 10^3$ fragments s^{-1}. If the shattered fragments are equally dispersed outside and inside the sampling tube, the fragmentation rate should be: $2 \times 174\ 10^3/900$ ∼400 fragments. This means that in the present case study (i.e. with the ice crystal size distribution displayed on Fig. 9a), the shattering effects will produce about 400 fragments on average per one equivalent irregular shaped ice crystal with a mean volume diameter of 310 µm. This value corresponds rather well to the results from Vidaurre and Hallett (2009, see their Fig. 6) from Cloudscope replicator data at 130 m s^{-1}. We note in passing that our results are within the order of magnitude given by Korolev et al. (2011), i.e. a number of fragments that may reach the order of 10^3, a number of fragments that intersect the probe's sample volume of a few hundred per shattered particle and the size of particle fragments as small as 10 µm.

According to our arguments, the slope of the CFSSP20-CCPI100 relationship on Fig. 8 is governed by the shattering efficiency via the fragmentation rate. Obviously, these values could be strongly dependent on the inlet design, the airspeed and the robustness of ice crystals via the impact kinetic energy to surface energy ratio providing the particle breakup (Vidaurre and Hallett, 2009). In the present case study, the ice crystals are mainly irregular shaped with evidence of vapour diffusion growth as shown with the examples displayed on Fig. 9b.

6 Conclusions

In this paper we analyzed cloud in situ measurements performed in boundary layer clouds during ASTAR2007 and POLACAT experiments. We show that in mixed phase clouds the FSSP measurements could be contaminated by ice crystals, inducing a wrong interpretation of the particle size and subsequent bulk parameters. Conversely, this contamination is revealed by a bimodal feature of the particle size distribution which could be a relevant indication of the presence of ice particles in mixed-phase clouds. The combined measurements of the FSSP and the Polar Nephelometer give a coherent

ACPD
12, 7909–7947, 2012

description of the effect of the ice crystals on the FSSP response. The FSSP particle size distributions are characterized by a bimodal shape with a second mode peaked between 25 and 35 µm related to ice crystals. The larger the amplitude of the second mode, the greater the ratio (REX) of extinction carried by ice particles to the total extinction (water droplets and ice crystals). The differences between the measured and theoretical (FSSP-100) phase functions at sideward scattering angles increase with REX values. This feature undoubtedly reveals the occurrence of aspherical particles. These observations have been extended to the combined data sets in mixed-phase clouds from ASTAR 2007 and POLARCAT experiments. A similar feature is observed with the FSSP-100 at airspeed up to 200 m s^{-1} and with the FSSP-300 series.

One sensitive aspect that could be considered is the probe size response to aspherical particles. In order to assess the size calibration for clouds of ice crystals the response of the FSSP-100 probe has been numerically simulated using a light scattering model of randomly oriented hexagonal ice particles and assuming both smooth and rough crystal surfaces. The results suggest that the second mode peaked between 25 µm and 35 µm does not represent true size responses but likely corresponds to bigger aspherical ice particles. This underestimation become extremely large if smooth crystal surfaces are considered. In our documented situation, measured Polar Nephelometer phase function suggest the presence of rough crystals, nevertheless, a sensitivity study would need to be done to conclude quantitatively. As for the number concentration measurements they are hampered by the unknown definition of the depth of field to aspherical randomly oriented ice crystals. There are no means of discriminating real and artefact ice particles related to the FSSP-100 secondary mode. However a literal interpretation of the cloud in situ measurements suggests that the FSSP-100 secondary mode peaked in the range 25–35 µm is likely to be due to the shattering of large ice crystals on the probe tips. This finding is supported by the rather good relationship between the number concentration of particles larger than 20 µm (hypothesized to be ice shattered-fragments measured by the FSSP) and the concentration of (natural) ice particles larger than 100 µm (CPI data). We may define the shattering

ACPD
12, 7909–7947, 2012

efficiency as the ratio of the measured ice shattered-fragments to the number of natural ice particles (with $d > 100\,\mu m$) impacting the probe leading edge. In the present study the shattering efficiency is evaluated to ∼7 %. It is found that about 400 ice fragments may result from the shattering of one equivalent irregular shaped ice crystal with a mean volume diameter of 310 µm. Obviously, these values could be strongly dependent on the inlet design, the airspeed and the robustness of ice crystals via the impact kinetic energy to surface energy ratio providing the particle breakup.

Acknowledgements. This work was funded by the Centre National d'Etudes Spatiales (CNES), the Institut Polaire Français Paul Emile Victor (IPEV), the Institut National des Sciences de l'Univers (INSU/CNRS) and the German Research Foundation (DFG, WE 1900/8-1). We thank the members of OPTIMARE GmbH, DLR (Deutsches Zentrum für Luft- und Raumfahrt) and Service des Avions Français Instrumentés pour la Recherche en Environnement (SAFIRE) who organize the experiment managements and aircraft operations. The ECMWF center is acknowledged for the reliable access to the forecasts and analysis. We acknowledge A. Herber (AWI), J. Pelon, K. Law (LATMOS), A. Schwarzenboeck and J.-F. Fournol (LaMP) for their active participation to the experiment. The authors are grateful to P. Yang for providing the IGOM code. We acknowledge K. James who reviewed the manuscript.

INSU
Institut national des sciences de l'Univers

The publication of this article is financed by CNRS-INSU.

References

Ashenden, R. and Marwitz, J. D.: Characterizing the supercooled large droplet environment with corresponding turboprop aircraft response, J. Aircraft, 35, 912–920, 1998.

Borrmann, S., Luo, B., and Mishchenko, M.: Application of the T-matrix method to the measurement of aspherical (ellipsoidal) particles with forward scattering optical particle counters, J. Aerosol Sci., 31, 789–799, 2000.

Baumgardner, D., Dye, J. E., Gandrud, B. W. and Knollenberg, R. G.:Interpretation of measurements made by the Forward Scattering Spectrometer Probe (FSSP-300) during the Airborne Arctic Stratospheric Expedition, J. Geophys. Res., 97, 8035–8046, 1992.

Baumgardner, D., Gayet, J.-F., Gerber, H., Korolev, A. V., and Twohy, C.: Clouds/Measurement Techniques In Situ, in: Encyclopedia of Atmospheric Sciences, edited by: Holton, J. R., Curry, J. A., and Pyle, J., Academic Press, London, 4000 pp., 2002.

Baumgardner, D., Brenguier, J.L., Bucholtz, A., Coe, H., DeMott, P., Garrett, T. J., Gayet, J. F., Hermann, M., Heymsfield, A., Korolev, A., Krämer, M., Petzold, A., Strapp, W., Pilewskie, P., Taylor, J., Twohy, C., Wendisch, M., Bachalo, W., and Chuang, P.: Airborne Measurements of Aerosol, Clouds and Radiation: A Cook's Tour of Mature and Emerging Technology, Atmos. Res., doi:10.1016/j.atmosres.2011.06.021, 2011.

Cober, S. G., Isaac, G. A., and Strapp, J. W.: Aircraft icing measurements in east coast winter storms, J. Appl. Meteor., 34, 88–100, 1995.

Cober, S. G., Korolev, A. V., Strapp, J. W., and Marcotte, D. L.: Measurements of aircraft icing environments which include supercooled large drops, 37th Aerospace Sci. Meeting, Reno, NV, AIAA Paper 99–0494, 1999.

Cober, S. G., Isaac, G. A., Korolev, A. V., and Strapp, J. W.: Assessing Cloud-Phase Conditions, J. Appl. Meteor., 40, 1967–1983, 2001.

Crépel, O., Gayet, J.-F., Fournol, J.-F. and Oshchepkov, S.: A new airborne Polar Nephelometer for the measurements of optical and microphysical cloud properties, Part II: Preliminary tests, Ann. Geophys., 15, 460–470, 1997.

Engvall, A.-C., Krejci, R., Ström, J., Treffeisen, R., Scheele, R., Hermansen, O., and Paatero, J.: Changes in aerosol properties during spring-summer period in the Arctic troposphere, Atmos. Chem. Phys., 8, 445–462, doi:10.5194/acp-8-445-2008, 2008.

Field, P. R., Wood, R., Brown, P. R. A., Kaye, P. H., Hirst, E.,Greenaway, R., and Smith, J. A.: Ice particle interarrival times measured with a Fast FSSP, J. Atmos. Sci., 20, 249–261, 2003.

Field, P. R., Heymsfield, A. J., and Bansemer, A.: Shattering and interarrival times measured by optical array probes in ice clouds, J. Atmos. Ocean. Tech., 23, 1357–1371, 2006.
Fugal, J. P. and Shaw, R. A.: Cloud particle size distributions measured with an airborne digital in-line holographic instrument, Atmos. Meas. Tech., 2, 259–271, doi:10.5194/amt-2-259-2009, 2009.
Gardiner, B. A. and Hallett, J.: Degradation of In-Cloud Forward Scattering Spectrometer Probe Measurements in the Presence of Ice Particles, J. Atmos. Ocean. Tech., 2, 171–180, 1985.
Garrett, T. J., Hobbs, P. V., and Gerber, H.: Shortwave, single-scattering properties of arctic ice clouds, J. Geophys. Res., 106, 15155–15172, 2001.
Gayet, J.-F., Febvre, G., and Larsen, H.: On the reliability of the PMS FSSP probe in the presence of small ice crystals, J. Atmos. Ocean. Tech., 13, 1300–1310, 1996.
Gayet, J. F., Crépel, O., Fournol, J. F., and Oshchepkov, S.: A new airborne polar Nephelometer for the measurements of optical and microphysical cloud properties. Part I: Theoretical design, Ann. Geophys., 15, 451–459, 1997.
Gayet, J.-F., Auriol. F., Oshchepkov. S., Schröder, F., Duroure, C., Febvre, G., Fournol, J.-F., Crépel, O., Personne, P., and Daugeron, D.: In situ measurements of the scattering phase function of stratocumulus, contrails and cirrus, Geophys. Res. Lett., 25, 971–974, 1998.
Gayet, J.-F., Asano, S., Yamazaki, A., Uchiyama, A., Sinyuk, A., Jourdan, O., and Auriol, F.: Two case studies of continental-type water and maritime mixed-phased stratocumuli over the sea. Part I : Microphysical and Optical propertie, J. Geophys. Res., 107, no. D21, doi:10.1029/2001JD001106, 2002.
Gayet, J.-F., Mioche, G., Dörnbrack, A., Ehrlich, A., Lampert, A., and Wendisch, M.: Microphysical and optical properties of Arctic mixed-phase clouds, The 9 April 2007 case study, Atmos. Chem. Phys., 9, 6581–6595, doi:10.5194/acp-9-6581-2009, 2009.
Gayet, J.-F., Shcherbakov, V., Voigt, C., Schumann, U., Schäuble, D., Jessberger, P., Petzold, A., Minikin, A., Schlager, H., Dubovik, O., Lapyonok, T., Krämer, M., and Kübbeler, M.: The evolution of microphysical and optical properties of an A380 contrail in the vortex phase, Atmos. Chem. Phys. Discuss., 11, 26867–26895, doi:10.5194/acpd-11-26867-2011, 2011.
Ivanova, D. C., Mitchell, D. L., Arnott, W. P., and Poellot, M.: A GCM parameterization for bimodal size spectra and ice mass removal rates in mid-latitude cirrus clouds, Atmos. Res., 59, 89–113, 2001.
Heymsfield, A. J.: On measurements of small ice particles in clouds, Geophys. Res. Lett., 34, L23812, doi:10.1029/2007GL030951, 2007.

ACPD
12, 7909–7947, 2012

Effects of ice crystals on the FSSP measurements in mixed phase clouds

G. Febvre et al.

Jensen, E. J., Lawson, P., Baker, B., Pilson, B., Mo, Q., Heymsfield, A. J., Bansemer, A., Bui, T.P., McGill, M., Hlavka, D., Heymsfield, G., Platnick, S., Arnold, G. T., and Tanelli, S.: On the importance of small ice crystals in tropical anvil cirrus, Atmos. Chem. Phys. Discuss., 9, 5321–5370, doi:10.5194/acpd-9-5321-2009, 2009.

Jourdan, O., Mioche, G., Garret, T. J., Schwarzenbock, A., Vidot, J., Xie, Y., Shcherbakov, V., Duroure, C., Yang, P., and Gayet, J.-F.: Coupling of the microphysical and optical properties of arctic clouds during the ASTAR 2004 experiment: Implications for light scattering modelling, J. Geophys. Res., 115, doi:10.1029/2010JD014016, 2010.

Knollenberg, R. G.: The optical array: An alternative to scattering or extinction for airborne particle size determination, J. Appl. Meteorol., 9, 86–103, 1970.

Knollenberg, R. G.: Techniques for probing cloud microstructure. Clouds: Their formation, optical properties and effects, edited by: Hobbs, P. V. and Deepak, A., Academic Press, 495 pp., 1981.

Korolev, A. V. and Isaac, G. A.: Shattering during sampling by OAPs and HVPS. Part I: Snow particles, J. Atmos. Ocean. Technol., 22, 528–543, 2005.

Korolev, A., Isaac, G. A., Cober, S. G., Strapp, J. W., and Hallett, J.: Microphysical charaterisation of mixed-phase clouds, Q. J. R. Meteorol. Soc., 129, 39–65, 2003.

Korolev, A., Emery, E., Strapp, W., Cober, S., Isaac, G., Wasey, M., and Cober, S. G.: Small ice particles in tropospheric clouds: fact or artifact?, Airborne Icing Instrumentation Evaluation Experiment, Bull. Amer. Meteor. Soc., 967–973, doi:10.1175/2010BAMS3141.1, 2011.

Law, K. S., Ancellet, G., Pelon, J., Turquety, S., Clerbaux, C., Pommier, M., de Villiers, R., Gayet, J.-F., Schwarzeboeck, A., Nedelec, P., Schneider, J., and Borrmann, S.: POLARCAT-France Airborne Experiment: first results, Intern. Global Atmospheric Chemistry conference (IGAC), Annecy, France, 7–12 September, 2008.

Lawson, R. P., Baker, B. A., and Schmitt, C. G.: An overview of microphysical properties of Arctic clouds observed in May and July 1998 during FIRE ACE, J. Geophys. Res., 106, 14989–15014, 2001.

Lawson, R. P., O'Connor, D., Zmarzly, P., Weaver, K., Baker, B. A., Mo, Q., and Jonsson, H.: The 2D-S (Stereo) probe: Design and preliminary tests of a new airborne, high-speed, high-resolution imaging probe, J. Atmos. Oceanic Technol., 23, 1462–1477, doi:10.1175/JTECH1927.1, 2006.

Lawson, R. P.: Effects of ice particles shattering on the 2D-S probe, Atmos. Meas. Tech., 4, 1361–1381, doi:10.5194/amt-4-1361-2011, 2011.

McFarquhar, G., Zhang, G., Poellot, M. R., Kok, G. L., McCoy, R., Tooman, T., Fridlind, A., and Heymsfield, A.: Ice properties of single-layer stratocumulus during the Mixed-Phase Arctic Cloud Experiment, J. Geophys. Res., 112, D24201, doi:10.1029/2007JD008633, 2007.

Miller, D., Ratvasky, T., Bernstein, B., McDonough, F., and Strapp, J. W.: NASA/FAA/NCAR supercooled large droplet icing flight research: Summary of winter 96–97 flight operations, AIAA 36th Aerospace Sci. Meeting and Exhibit, Reno, NV, AIAA Paper 98–0577, 1998.

Mishchenko, M. I., Travis, L. D., Kahn, R. A., and West, R. A.: Modeling phase functions for dustlike tropospheric aerosols using a shape mixture of randomly oriented polydisperse spheroids, J. Geophys. Res., 102, 16831–16847, 1997.

Mitchell, D. L., Arnott, W. P., Schmitt, C., Lowenthal, D., and Edwards, J. M.: A fundamental difference between ice crystal and cloud droplet absorption: photon tunneling effects. 10th Conference on Atmospheric Radiation: A Symposium with Tributes to the Works of Verner E. Suomi, AMS, Madison, WI, 28 June–2 July 1999.

Nagel, D., Maixner, U., Strapp, W., and Wasey, M.: Advancements in Techniques for Calibration and Characterization of In Situ Optical Particle Measuring Probes, and Applications to the FSSP-100 Probe, J. Atmos. Ocean Tech., 24, 745–760, 2007.

Niu, J., Carey, L. D., Yang, P., and Vonder Haar, T. H.: Optical properties of a vertically inhomogeneous mid-latitude mid-level mixed-phase altocumulus in the infrared region, Atmos. Res., 88, 234–242, 2008.

Pinnick, R. G., Garvey, D. M., and Duncan, L. D.: Calibration of Knollenberg FSSP Light-Scattering Counters for Measurement of Cloud Droplets, J. Appl. Meteorol., 20, 9, 1049–1057, 1981.

Protat, A., McFarquhar, G., Um, J., and Delanoë, J.: Obtaining best estimates for the microphysical and radiative properties of tropical ice clouds from TWP-ICE in-situ microphysical observations, J. Appl. Meteorol. Clim., 50, 895–915, doi:10.1175/2010JAMC2401.1, 2010.

Riley, J. T.: Mixed-phase icing conditions: A review. Airport and Aircraft Safety Research and Development Rep. DOT/ FAA/AR-98/76, Federal Aviation Administration, Atlantic City, NJ, 45 pp., 1998.

Sassen, K. and Liou, K. N.: Scattering and polarized laser light by water droplets, mixed- phase and ice crystal clouds. Part I : Angular scattering patterns, J. Atmos. Sci., 36, 838–851, 1979.

Shcherbakov, V., Gayet, J.-F., Jourdan, O., Ström, J., and Minikin, A.: Light scattering by single ice crystals of cirrus clouds, Geophys. Res. Lett., 33, L15809, doi:10.1029/2006GL026055, 2006.

ACPD

12, 7909–7947, 2012

Effects of ice crystals on the FSSP measurements in mixed phase clouds

G. Febvre et al.

Shcherbakov, V., Gayet, J.-F., Febvre, G., Heymsfield, A. J., and Mioche, G.: Probabilistic model of shattering effect on in-cloud measurements, Atmos. Chem. Phys. Discuss., 10, 11009–11045, doi:10.5194/acpd-10-11009-2010, 2010.

Vidaurre, G. and Hallett, J.: Particle Impact and Breakup in Aircraft Measurement, J. Atmos. Ocean Technol., 26, 972–983, doi:10.1175/2008JTECHA1147.1, 2009.

Warren, S. G. and Brandt, R. E.: Optical constants of ice from the ultraviolet to the microwave: A revised compilation, J. Geophys. Res., 113, D14220, doi:10.1029/2007JD009744, 2008.

Yang, P. and Liou, K. N.: Geometric-optics-integral-equation method for light scattering by non-spherical ice crystals, Appl. Opt., 35, 6568–6584, 1996.

Yang, P. and Liou, K. N.: Single-scattering properties of complex ice crystals in terrestrial atmosphere, Contrib. Atmos. Phys., 71, 223–248, 1998.

Zhang, Z., Yang, P., Kattawar, G. W., and Wiscombe, W. J.: Single-scattering properties of Platonic solids in geometrical-optics regime, J. Q. S. R. Trans., 106, 595–603, 2007.

Table 1. Mean values of the cloud parameters over the times-sequences labelled a to d on Fig. 1. The parameters are the temperature, the liquid water content, the mean volume diameter, the asymmetry parameter, the CPI on PN extinctions ratio (REX) and the concentration of ice particles (with $d > 100\,\mu m$).

Sequence	T (°C)	LWC ($g\,m^{-3}$)	MVD (µm)	g	REX ratio (Ext CPI/Ext NP)	C100 (l^{-1})
a	−19.2	0.23	14.7	0.843	0.03	8.9
b	−17.4	0.04	13.6	0.828	0.10	4.9
c	−17.1	0.03	19.0	0.803	0.36	12.9
d	−14.0	0.02	33.7	0.769	0.80	12.1

ACPD
12, 7909–7947, 2012

Table 2. Bin limit sizes for the FSSP-100 particle counter for water droplets (Mie calculations) and from hexagonal particles modelling for the refractive index of ice (1.31) assuming particles having a mean aspect ratio of 0.5. Results are reported for the nominal and extended size ranges.

Nominal Range: 3–45 mm									
Channel no.	Water droplets (Mie)			Rought Hexagonal ice particles			Smooth Hexagonal ice particles		
	min	median	max	min	median	max	min	median	max
1	1.5	3	4.5	2.0	3.4	4.8	1.6	3.8	6.4
2	4.5	6	7.5	4.8	6.2	7.5	6.4	9.2	12.1
3	7.5	9	10.5	7.5	8.9	10.3	12.1	15.2	18.5
4	10.5	12	13.5	10.3	11.7	13.1	18.5	21.9	25.4
5	13.5	15	16.5	13.1	14.5	15.9	25.4	28.9	32.6
6	16.5	18	19.5	15.9	17.3	18.6	32.6	36.4	40.2
7	19.5	21	22.5	18.6	20.0	21.4	40.2	44.1	48.1
8	22.5	24	25.5	21.4	22.8	24.2	48.1	52.2	56.3
9	25.5	27	28.5	24.2	25.6	27.0	56.3	60.5	64.8
10	28.5	30	31.5	27.0	28.4	29.8	64.8	69.1	73.4
11	31.5	33	34.5	29.8	31.1	32.5	73.4	77.8	82.3
12	34.5	36	37.5	32.5	33.9	35.3	82.3	86.8	91.4
13	37.5	39	40.5	35.3	36.7	38.1	91.4	96.0	100.6
14	40.5	42	43.5	38.1	39.5	40.9	100.6	105.3	110.1
15	43.5	45	46.5	40.9	42.3	43.6	110.1	114.9	119.7

Table 2. Continued.

Extended Range: 6–90 mm									
Channel no.	Water droplets (Mie)			Hexagonal ice particles			Smooth Hexagonal ice particles		
	min	median	max	min	median	max	min	median	max
1	3	6	9	3.4	6.2	8.9	3.8	9.2	15.2
2	9	12	15	8.9	11.7	14.5	15.2	21.9	28.9
3	15	18	21	14.5	17.3	20.0	28.9	36.4	44.1
4	21	24	27	20.0	22.8	25.6	44.1	52.2	60.5
5	27	30	33	25.6	28.4	31.1	60.5	69.1	77.8
6	33	36	39	31.1	33.9	36.7	77.8	86.8	96.0
7	39	42	45	36.7	39.5	42.3	96.0	105.3	114.9
8	45	48	51	42.3	45.0	47.8	114.9	124.5	134.4
9	51	54	57	47.8	50.6	53.4	134.4	144.4	154.5
10	57	60	63	53.4	56.1	58.9	154.5	164.8	175.2
11	63	66	69	58.9	61.7	64.5	175.2	185.7	196.4
12	69	72	75	64.5	67.2	70.0	196.4	207.1	218.0
13	75	78	81	70.0	72.8	75.6	218.0	229.0	240.1
14	81	84	87	75.6	78.4	81.1	240.1	251.3	262.6
15	87	90	93	81.1	83.9	86.7	262.6	274.1	285.6

ACPD
12, 7909–7947, 2012

Effects of ice crystals on the FSSP measurements in mixed phase clouds

G. Febvre et al.

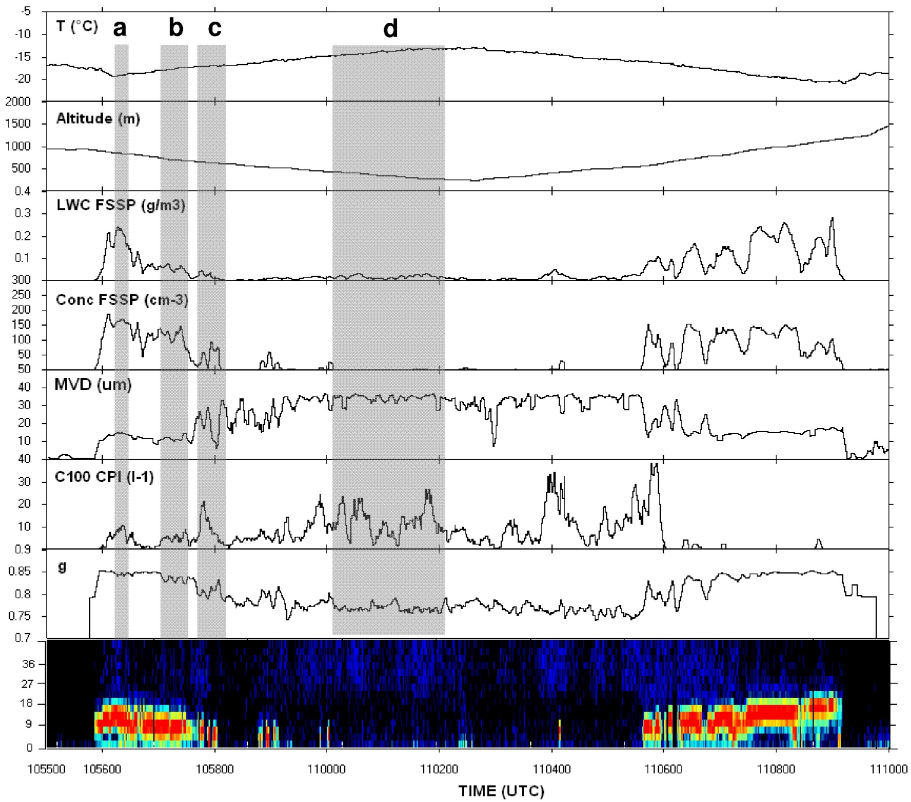

Fig. 1. Time-series of cloud parameters measured during a descent-climbing sequence in the mixed-phase stratiform cloud layer (ASTAR, 8 April 2007 case study). The parameters (plotted at 1 Hz) are the following: the air temperature, altitude, droplet concentration, liquid water content (LWC) and mean volume diameter (MVD), the concentration of ice particles larger than 100 µm ($C100$), the asymmetry parameter (g) and the FSSP size distribution represented with colour-scaled to the particle concentration.

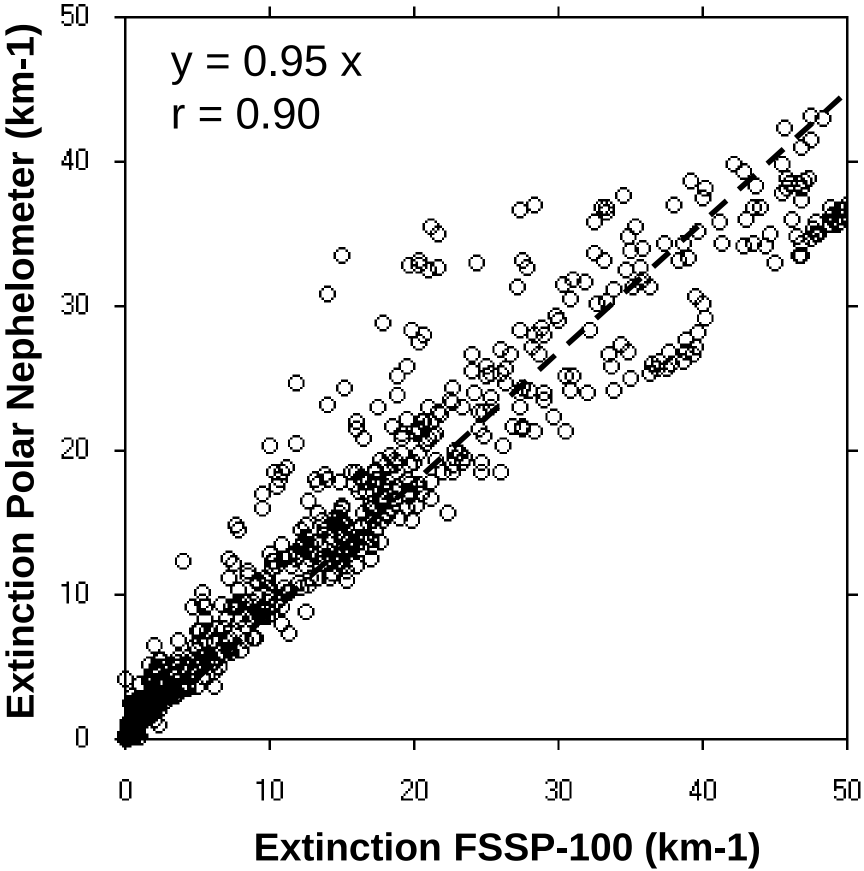

Fig. 2. Relationship between the extinction measurements from the Polar Nephelometer and the FSSP-100. The data correspond to cloud liquid water only (i.e. $g > 0.83$). ASTAR, 8 April 2007 case study.

ACPD
12, 7909–7947, 2012

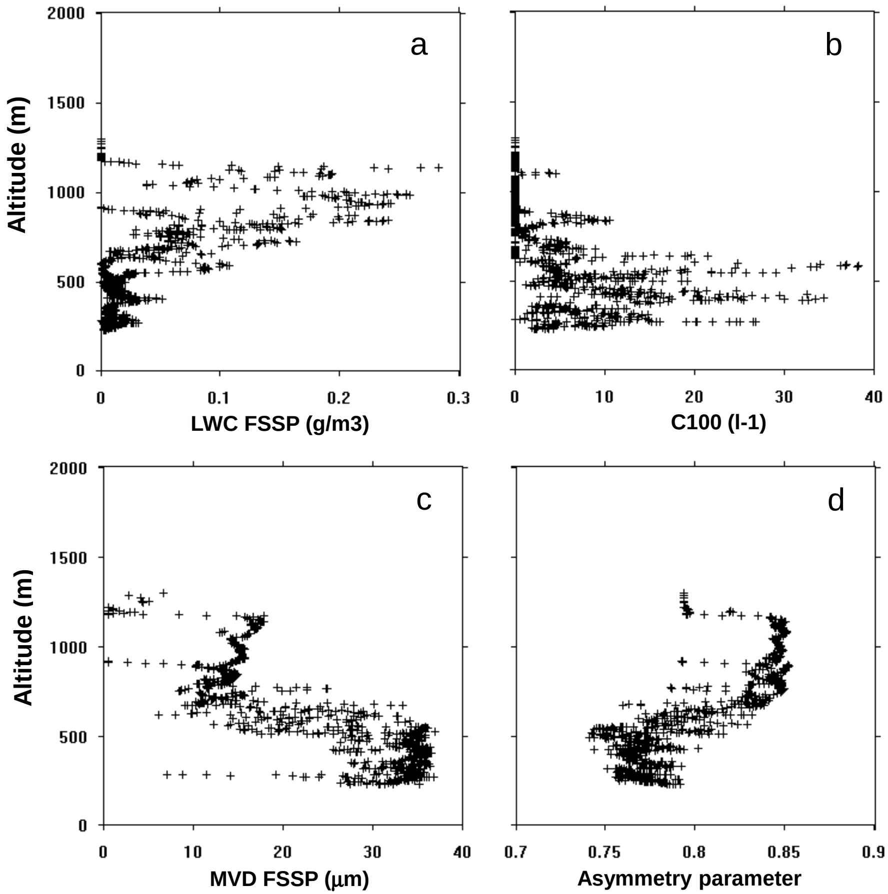

Fig. 3. Vertical profiles of cloud parameters obtained during the descent-climbing sequence on Fig. 1. **(a)**: liquid water content; **(b)**: concentration of ice particles with $d > 100\,\mu\text{m}$; **(c)**: mean volume diameter and **(d)**: asymmetry parameter.

ACPD
12, 7909–7947, 2012

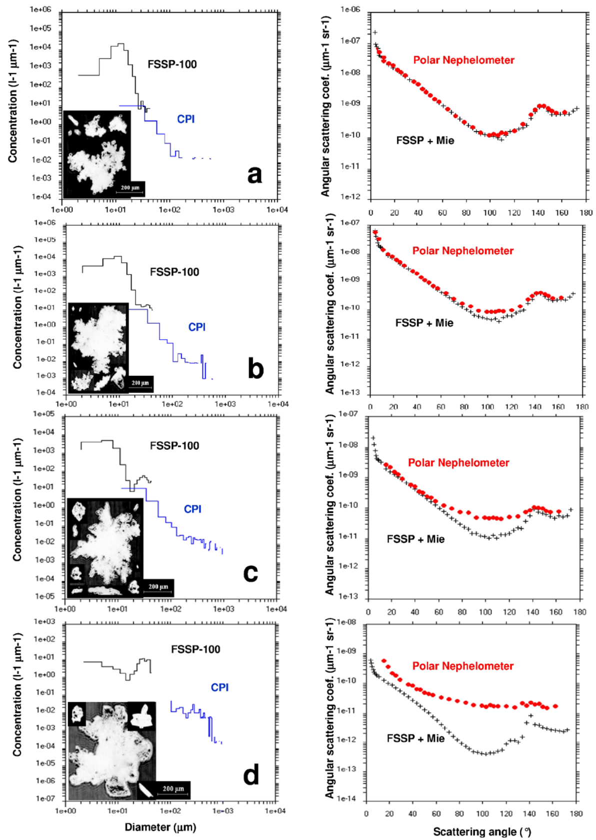

Fig. 4. Results obtained for the four cloud sequences labelled (a), (b), (c) and (d) on Fig. 1. Left panels: mean particle size distributions from FSSP and CPI measurements with examples of ice crystal images. Right panels: mean measured scattering phase function (Polar Nephelometer with red dots symbols). The theoretical phase functions are calculated from the FSSP data with the Mie theory and plotted with black cross symbols.

ACPD
12, 7909–7947, 2012

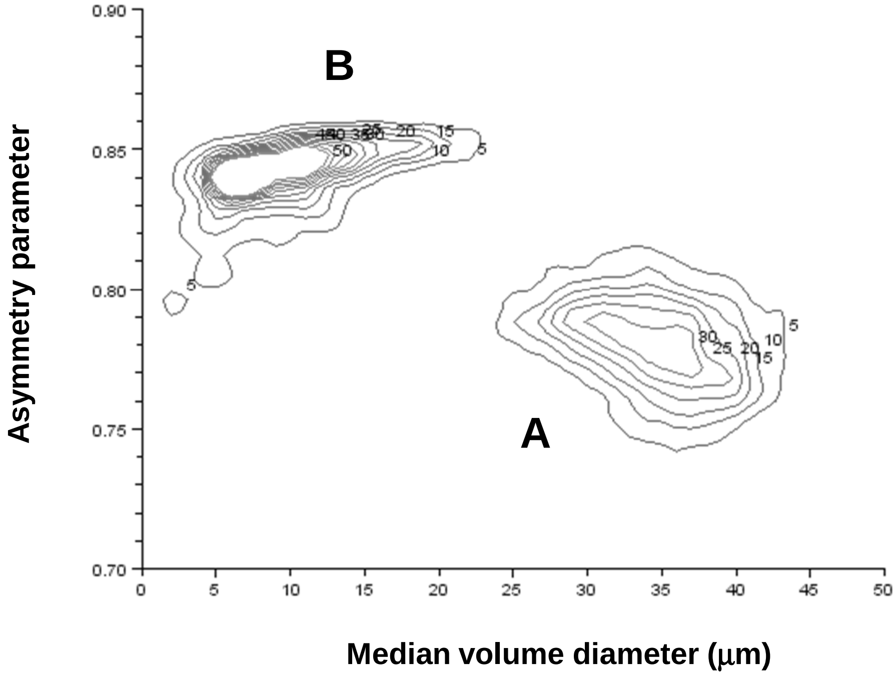

Fig. 5. Mean volume diameter – asymmetry scatter plots of the FSSP-100 and Polar Nephelometer measurements obtained in mixed-phase clouds during ASTAR and POLARCAT experiments (~30 000 data). The number of observations are represented by iso-lines.

ACPD
12, 7909–7947, 2012

Effects of ice crystals on the FSSP measurements in mixed phase clouds

G. Febvre et al.

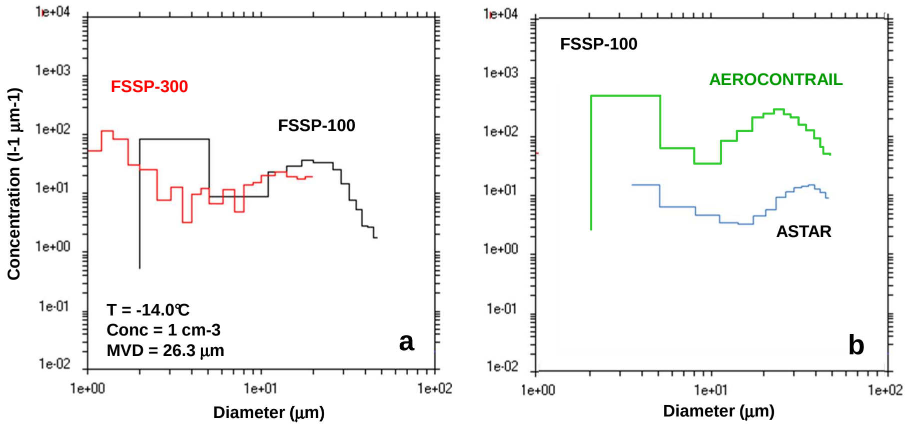

Fig. 6. (a): composite representation of the particle size distributions measured simultaneously by the FSSP-100 and the FSSP-300 in mixed phase clouds during the POLARCAT experiment (12 July 2008). **(b)**: composite representation of the particle size distributions measured by the FSSP-100 during ASTAR with an airspeed of 100 m s^{-1} and during AEROCONTRAIL with an airspeed of 200 m s^{-1}.

ACPD
12, 7909–7947, 2012

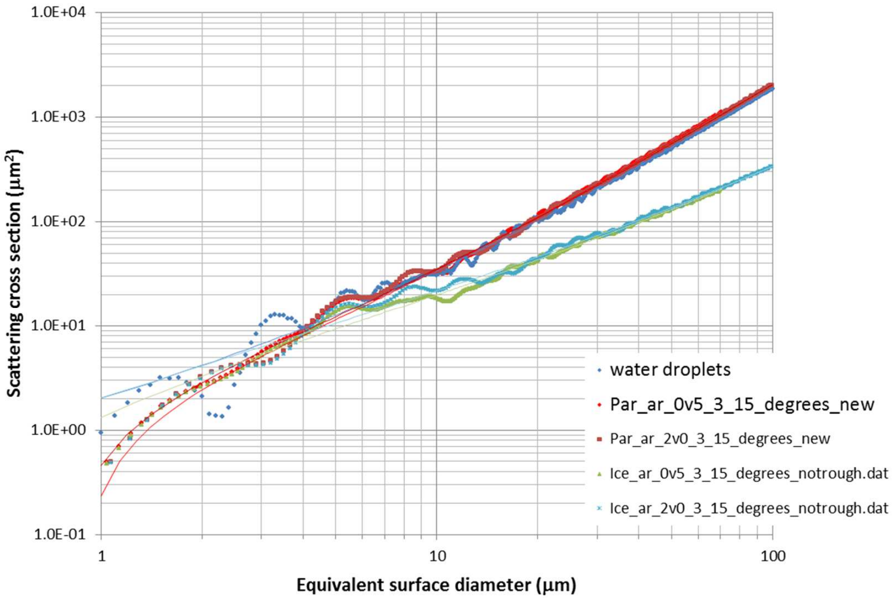

Fig. 7. The scattering cross sections for the FSSP-100 as function of particle size obtained from hexagonal ice particle (aspect ratio of 2) calculations with averaging over all orientations (red curve). The Mie theory calculations (blue line) for water droplets are also reported. Both curves are for HeNe laser light ($\lambda = 632.8$ nm) and the FSSP-100 scattering geometry (3°–15°). The thin lines represent the best fits of the theoretical results (water droplets and ice crystals) from which the bin limit sizes have been defined (see Table 2).

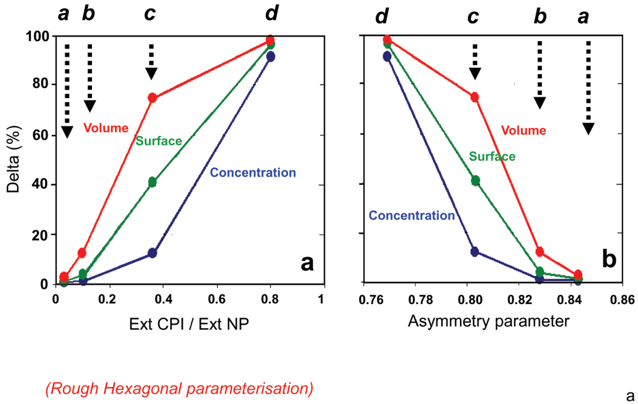

a

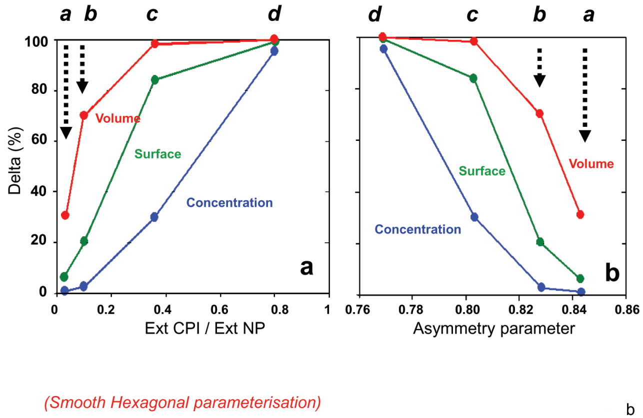

b

Fig. 8. Relative contribution of the ice particles (DELTA values) on number concentration, extinction (surface) and liquid/ice water content (volume) measurements as a function of: the REX extinction ratio (CPI data to PN measurements) andthe asymmetry parameter, respectively. The data have been obtained during the cloud sequences labelled **(a)**, **(b)**, **(c)** and **(d)** (see Fig. 1). (1) Rough hexagonal crystals simulation (2) Smooth hexagonal crystals simulation

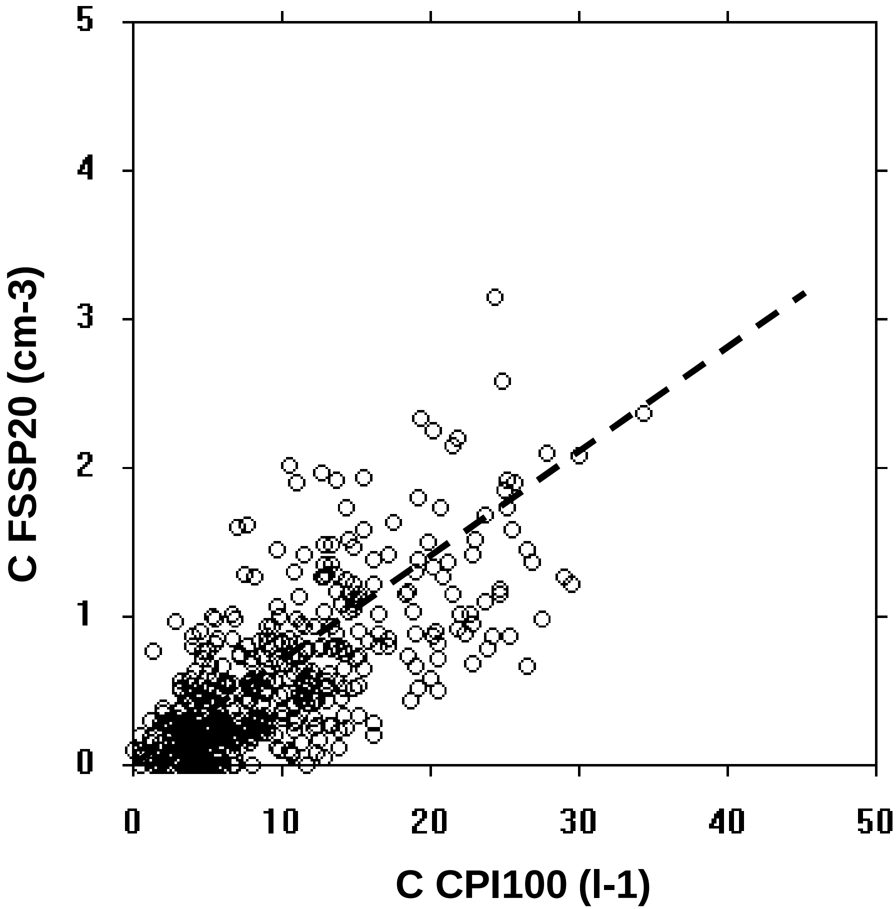

Fig. 9. Number concentration of ice crystals ($d > 20\,\mu m$) measured by the FSSP-100 versus the concentration of ice particles ($d > 100\,\mu m$) measured with the CPI (ASTAR, 8 April 2007).

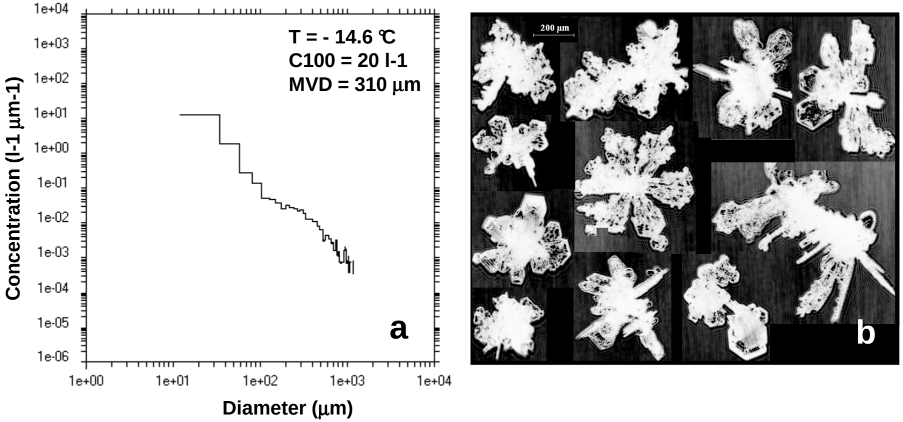

Fig. 10. (a) Particle size distribution measured by the CPI during the sequence between 10:58 and 11:06 UTC on Fig. 1 ($T = -14.6\,^{\circ}\mathrm{C}$). **(b)**: examples of ice crystal images measured by the CPI during this sequence.

ACPD
12, 7909–7947, 2012